

This article was downloaded by:

On: 26 January 2011

Access details: *Access Details: Free Access*

Publisher *Taylor & Francis*

Informa Ltd Registered in England and Wales Registered Number: 1072954 Registered office: Mortimer House, 37-41 Mortimer Street, London W1T 3JH, UK



Liquid Crystals

Publication details, including instructions for authors and subscription information:

<http://www.informaworld.com/smpp/title~content=t713926090>

Characterization by mirage effect technique of dye diffusion in columnar discotic liquid crystals

M. Daoud^a; G. Louis^b; X. Quélin^b; M. Gharbia^c; A. Gharbi^c; P. Peretti^d

^a Ecole Supérieure des Sciences et Techniques de Tunis, Tunis, Tunisie ^b Département de Recherches Physiques (URA CNRS 71), Université Paris 6, Paris cedex 5, France ^c Laboratoire de Cristaux Liquides et Polymères, Faculté des Sciences, Tunis, Tunisie ^d Groupe de Recherche en Physique et Biophysique (EA 228), Université Paris 5, Paris cedex 6, France

To cite this Article Daoud, M. , Louis, G. , Quélin, X. , Gharbia, M. , Gharbi, A. and Peretti, P.(1995) 'Characterization by mirage effect technique of dye diffusion in columnar discotic liquid crystals', *Liquid Crystals*, 19: 6, 833 – 837

To link to this Article: DOI: 10.1080/02678299508031107

URL: <http://dx.doi.org/10.1080/02678299508031107>

PLEASE SCROLL DOWN FOR ARTICLE

Full terms and conditions of use: <http://www.informaworld.com/terms-and-conditions-of-access.pdf>

This article may be used for research, teaching and private study purposes. Any substantial or systematic reproduction, re-distribution, re-selling, loan or sub-licensing, systematic supply or distribution in any form to anyone is expressly forbidden.

The publisher does not give any warranty express or implied or make any representation that the contents will be complete or accurate or up to date. The accuracy of any instructions, formulae and drug doses should be independently verified with primary sources. The publisher shall not be liable for any loss, actions, claims, proceedings, demand or costs or damages whatsoever or howsoever caused arising directly or indirectly in connection with or arising out of the use of this material.

Characterization by mirage effect technique of dye diffusion in columnar discotic liquid crystals

by M. DAOUD*†, G. LOUIS‡, X. QUÉLIN‡, M. GHARBI§,
A. GHARBI§ and P. PERETTI¶

† Ecole Supérieure des Sciences et Techniques de Tunis,
Groupe des Cristaux Liquides, 5 avenue Taha Hussein, B.P. 56,
Bab Menara, 1008, Tunis, Tunisie

‡ Université Paris 6, Département de Recherches Physiques (URA CNRS 71),
Tour 22, 4 place Jussieu, 75252 Paris cedex 5, France

§ Laboratoire de Cristaux Liquides et Polymères, Faculté des Sciences,
Tunis, Tunisie

¶ Université Paris 5, Groupe de Recherche en Physique et Biophysique (EA 228),
45 rue des Saints-Pères, 75270 Paris cedex 6, France

(Received 22 February 1995; in final form 7 July 1995; accepted 7 July 1995)

The anisotropic behaviour of the matter diffusion in columnar discotic liquid crystals is studied by the 'mirage effect' technique. The D_h and D_0 mesophases of C_8 HET and C_{11} HET, respectively, are considered. The impurity (a dye, the 1-[4-(xylyloxy)xylyloxy]-2-naphthol) diffusing in these mesophases is detected by the photothermal deflection technique. Measurements of the diffusion coefficients are performed in two perpendicular directions, along and perpendicularly to the molecular columns. Effects of impurity size, length and type of the branched chains on the discs of triphenylene, and molecule stackings in columns, are presented.

1. Introduction

In previous papers [1, 2] we have demonstrated that an optical method, based on the detection of the transmitted light through the material, is well-suited to measure diffusion coefficients in columnar discotic liquid crystals. In the present work, we involve a photothermal probe-beam deflection technique (or 'mirage effect' technique), which is only sensitive to the light energy absorbed by the material under study. This method was first introduced by Boccara *et al.* [3] and has since then proved to be a useful tool in the study of optical [4] and thermal properties [5] of materials. The photothermal technique is now of interest in the field of thermal imaging [6]. Concerning liquid crystals, we have shown the accuracy of this technique to detect phase transitions [7] and to characterize anisotropic behaviour of thermal diffusivity in a discotic hexagonal ordered phase [8].

The aim of this work is to demonstrate that the photothermal deflection method can be a useful technique to measure, in different directions, dye diffusion coefficients in ordered mesophases of liquid crystals.

In such a technique, a modulated light beam (pump beam) illuminates the sample under study. As a result of

radiationless processes, light is converted into heat, which induces thermoelastic waves in the sample. For low frequency modulation range (< 10 Hz), one can assume that there is no contribution of the acoustical mode to the thermal field. The heat flow within the sample produces a refractive index gradient in the adjacent medium close to the sample surface. A second laser beam (probe beam), directed through the gradient in the adjacent medium and parallel to the sample surface, is then deflected by the 'mirage effect'. The analysis of the deflection angle leads to the optical and thermal properties of the sample. The evolution of optical absorption coefficient is analysed and related to the concentration of dye molecules diffusing in hexagonal columnar discotic liquid crystals.

We have measured the diffusion coefficients D_{\parallel} and D_{\perp} in two configurations, along and perpendicular to the columns. We have shown that the ratio $r = D_{\parallel}/D_{\perp}$ is superior to 1 and is a function of the temperature, of the impurity size, of the length and type of branched chains on the discs of triphenylene, and of the kind of the molecules stacking in the columns.

2. Theory

A three-dimensional thermal conduction model is used for the photothermal deflection theory. The geometry for

* Author for correspondence.

the theoretical analysis, is described in figure 1. In the reference frame, the thermal field $T(x, y, z, t)$ is determined according to energy conservation law by the 3D thermal conduction equation in an anisotropic medium [9]:

$$\kappa \nabla^2 T(x, y, z, t) + g(x, y, z, t) = \rho C_p \frac{\partial T(x, y, z, t)}{\partial t} \quad (1)$$

where ρ and C_p are the density and the specific heat of the sample, respectively. The quantity $g(x, y, z, t)$ denotes the thermal energy deposited by the pump beam per unit time and unit volume.

The expressions of the thermal conductivity tensor κ , for the normally oriented areas and planar configurations, are reported in table 1.

Expressions of stationary solutions of this differential equation for a frequency modulation $f = \omega/2\pi$ of incident light beam are

$$T(x, y, z, t) = \tau(x, y, z) \exp(i\omega t). \quad (2)$$

Assuming a Gaussian profile of the pump-beam light energy, equation (1) becomes

$$\kappa \nabla^2 \tau(x, y, z) - i\rho C_p \omega \tau = -\frac{2\beta I_0}{\pi r_g^2} \exp\left[-\frac{2(x^2 + y^2)}{r_g^2}\right] \times \exp(-\beta z) \quad (3)$$

where I_0 is the power of the pump beam, r_g its radius, and β the optical-absorption-rate constant of the sample.

In the surrounding media, front and rear, equation (1) can also be written with $g(x, y, z, t) = 0$ as they do not absorb the incident light energy, and $\kappa = \kappa$, because of their isotropic thermal behaviour

$$\kappa_i \nabla^2 \tau_i(x, y, z) = i\rho_i C_p^i \omega \tau_i(x, y, z) \quad (4)$$

where $i = f$ for the front medium, and $i = b$ for the backing one.

In order to obtain the temperature distribution τ_i in the three media, we used a 2D Fourier transform [10, 11] in the (x, y) plane, taking account of the boundary conditions at the interfaces (continuity of temperature and heat flow) between the sample and the two adjacent media.

The magnitude and direction of the probe beam deflection ϕ are determined by the periodic gradient of the temperature in the front medium and are given by the line integral

$$\phi = -\frac{1}{n} \frac{dn}{dT} \int_L \nabla \tau_f \wedge d\mathbf{l}, \quad (5)$$

where n is the refractive index of the front medium, L the probe-beam path and $d\mathbf{l}$ an incremental distance along L . When the probe and the pump beams are exactly crossing above the surface of the sample, this deflection leads to the unique normal component ϕ_n :

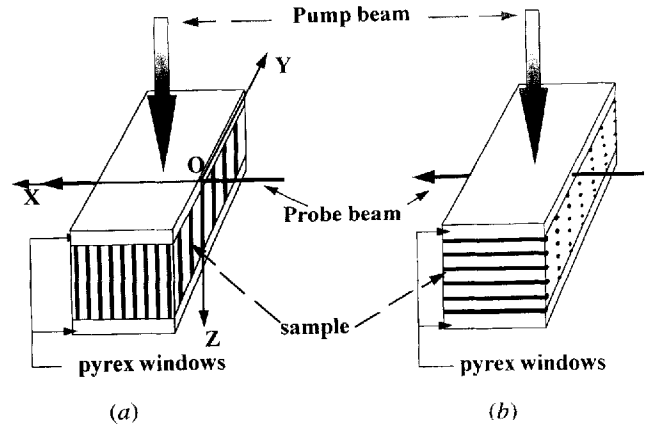


Figure 1. Schematic diagram of the oriented molecular columns between pyrex plates in the (X, Y, Z) reference frame: (a) homeotropic orientation and (b) planar orientation.

Table 1. In these expressions, κ_{\perp} and κ_{\parallel} denote the thermal conductivity coefficients in a direction perpendicular and parallel to the molecular columns, respectively.

Configuration	Thermal conductivity tensor
Normally oriented areas configuration (see figure 1 (a))	$\kappa_h = \begin{pmatrix} \kappa_{\perp} & 0 & 0 \\ 0 & \kappa_{\perp} & 0 \\ 0 & 0 & \kappa_{\parallel} \end{pmatrix}$
Planar configuration (see figure 1 (b))	$\kappa_p = \begin{pmatrix} \kappa_{\perp} & 0 & 0 \\ 0 & \kappa_{\parallel} & 0 \\ 0 & 0 & \kappa_{\perp} \end{pmatrix}$

$$\phi_n \propto \int_{-\infty}^{+\infty} \frac{\partial \tau_f}{\partial z} dx. \quad (6)$$

The resolution of the differential thermal conduction equation in the wavevector space leads us, by the inverse Fourier transform, to the expression of τ_f . In our modulation frequency range (≤ 10 Hz), the sample is much larger than the thermal diffusion length $l_f = (2\kappa_f/\rho_f C_p^f \omega)^{1/2}$. So the sample in the (x, y) plane can be considered as infinite. The integral (equation (6)) will be calculated on a few thermal wavelengths interval. We have verified by a numerical simulation, for different values of liquid crystals thermal conductivity and modulation frequency, the proportionality between ϕ_n and β , as it was predicted [12] as long as the sample remains optically thin. As the liquid crystal sample does not absorb the incident light, the evolution of ϕ_n and consequently β , is directly related to the dye concentration located along the pump beam path. Diffusion of the dye in the sample is determined by the analysis of ϕ_n versus time for a given

position x of the pump beam, or versus various x positions of the pump beam for a given time.

A 1D treatment of the molecular diffusion processes is available as shown in photography of the dye diffusion in the C₈HET columnar hexagonal phase (see figure 4 of [1]).

For the 1D case, the dye concentration $C(x, t)$ is then related to the diffusion coefficient D according to the second Fick's law

$$\frac{\partial C(x, t)}{\partial t} = D \frac{\partial^2 C(x, t)}{\partial x^2}. \quad (7)$$

This equation agrees with the following solution

$$C(x, t) = C(0, t) \exp\left(-\frac{x^2}{4Dt}\right). \quad (8)$$

The concentration at the origin $C(0, t)$ is given by a relationship

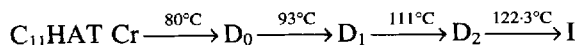
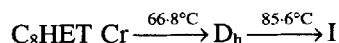
$$C(0, t) = \frac{Q}{(\pi Dt)^{1/2}}$$

where Q is the amount of dye molecules deposited per unit area.

3. Experimental

The columnar disc-like mesogens were synthesized by Destrade *et al.* [13]. The molecules (see figure 2) present a central core of triphenylene to which six lateral chains are bound by ether or ester groups.

The samples, the hexa-*n*-ethoxytriphenylene (C₈HET) and the hexa-*n*-dodecanoate of triphenylene (C₁₁HAT), respectively, exhibit the following stable phases:



Experiments are performed in the D₀ phase of the C₁₁HAT and the D_h phase of the C₈HET, where the lattice of the columns is hexagonal. Furthermore, the molecules are regularly stacked in columns with an intermolecular spacing equal to 0.36 nm. The distance between two adjacent columns increases with the length chains. It is

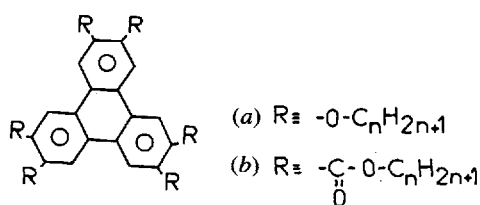


Figure 2. Chemical formulas of columnar discotic molecules: (a) the hexa-*n*-ethoxytriphenylene (C₈HET) and (b) the hexa-*n*-dodecanoate of triphenylene (C₁₁HAT).

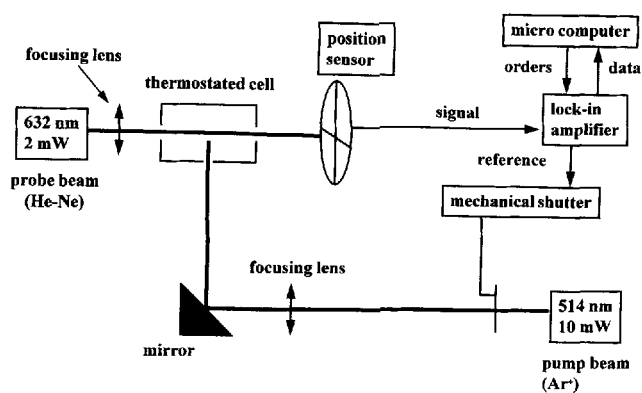


Figure 3. Experimental set-up.

estimated to 2.22 nm for the C₈HET and to 2.66 nm for the C₁₁HAT [14].

The impurity diffusing in these phases is a Red Oil O, biological stain, certified [1320-06-5], the 1-[4-xylyl-azo]xylylazo]-2-naphthol (dye content ~85 per cent), which presents a melting point $T_f = 120^\circ\text{C}$ and a maximum absorption wavelength situated at $\lambda = 518 \text{ nm}$ (Aldrich).

The block diagram of the experimental set-up is shown in figure 3. A 8 mW power Argon laser, tuned on a 488 nm wavelength, provides a Gaussian pump beam focused on the sample surface. The low frequency modulation in the 1–10 Hz range, is ensured by an electromechanical shutter (NM Laser Products LS200). The probe beam is a 2 mW power He-Ne laser beam focused in the interaction region by the mean of a 10 cm focusing lens. The deflection angle (a few milliradians) is detected by a photoelectric position sensor (Centronic QD50) and measured by a lock-in amplifier (PAR 5206). Data were collected and analysed by a personal computer. The sample holder is placed in a thermostated cell (see figure 4). The temperature regulation is monitored by a microprocessor (Coreci

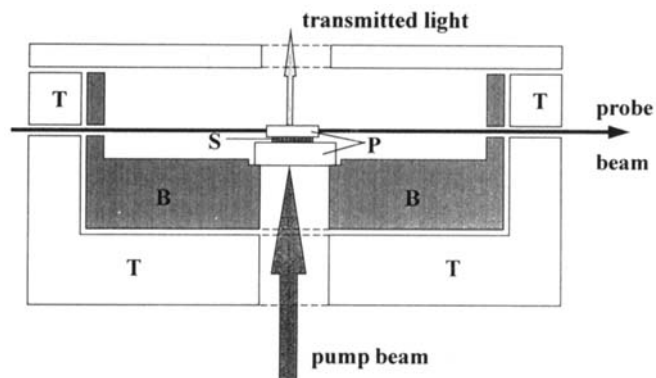


Figure 4. Schematic diagram of the thermostated cell. Letters refer as follows: B for the brass thermo-electric heater, T for the teflon insulator, S for the sample and P for the pyrex holders.

MCF/RNZ), which ensure that the average temperature is adjusted by 20 to 150°C, with an accuracy of 0.2°C. The temperature is measured by means of a platinum resistor in contact with the thermostated cell.

We have used the same experimental technique as the one described in [1] for the sample thickness and glass plates preparation, for the annealing between two transitions, and for the orientation of molecular columns in the two configurations, columns parallel to the plates (planar) or perpendicular to them (homeotropic).

4. Results and discussion

We present the measurements of D_{\parallel} and D_{\perp} diffusion coefficients of the red dye, in the D_h (C_8 HET) and the D_0 (C_{11} HAT) hexagonal columnar discotic phases, for two perpendicular directions, along and perpendicularly to the molecular columns.

The study of the dye concentration $C(x, t)$ versus x leads to the half of the bell curve (see figure 5) according to equation (8) which shows that the matter diffusion in hexagonal columnar discotic liquid crystals is well-described by the second Fick's law.

In order to determine the diffusion coefficient values, a logarithmic representation of the data is suitable. From the slope of $\ln [C(0, t)/C(x, t)]$ versus $1/t$ at a given position x (see figure 6), or versus x^2 at a given time t (see figure 7), we can deduce the diffusion coefficients D_{\perp} and D_{\parallel} reported in table 2. Because the dye position x is determined with an accuracy of 0.05 mm due to the pump beam diameter, our measurements are given with a precision about 10 per cent.

Values of the diffusion coefficients, obtained by an

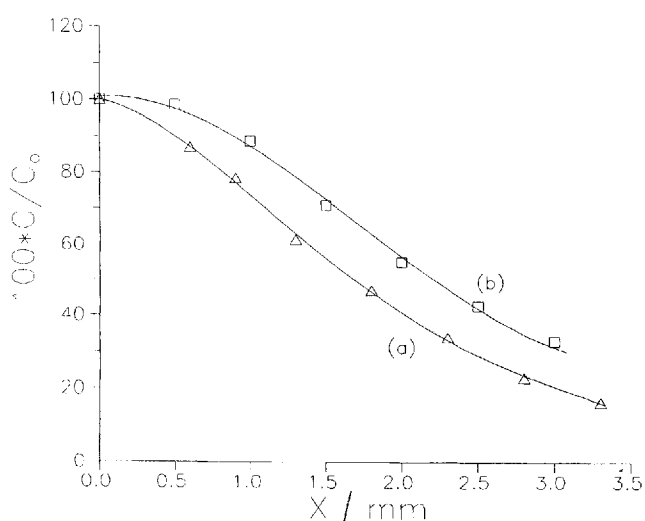


Figure 5. Relative evolution of the red dye concentration versus x position: (a) in planar orientation of C_8 HET ($T = 75^\circ\text{C}$) at $t = 18$ h 30 min and (b) in homeotropic orientation of C_8 HET ($T = 75^\circ\text{C}$) at $t = 40$ h.

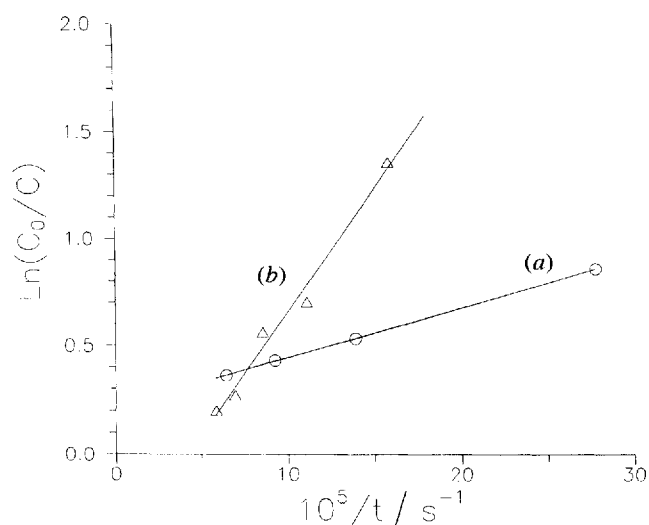


Figure 6. Plot of $\ln [C(0, t)/C(x, t)]$ as a function of $1/t$ for the red dye diffusion. (a) in planar orientation of C_{11} HAT ($T = 90^\circ\text{C}$) at $x = 1$ mm and (b) in homeotropic orientation of C_{11} HAT ($T = 90^\circ\text{C}$) at $x = 1.45$ mm.

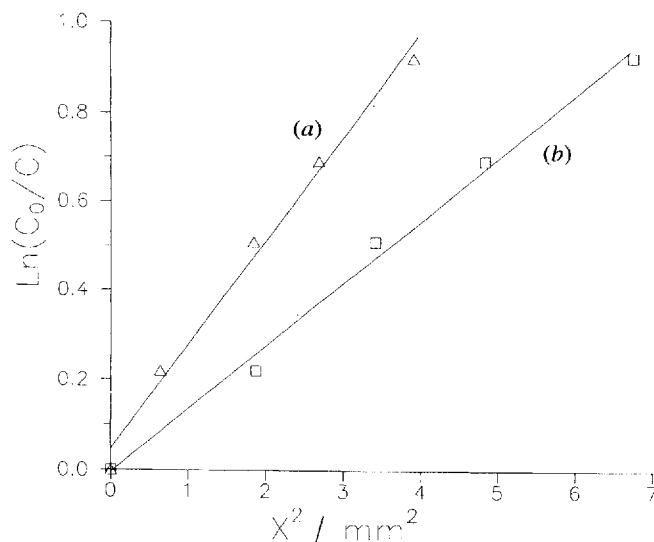


Figure 7. Plot of $\ln [C(0, t)/C(x, t)]$ as a function of x^2 for the red dye diffusion. (a) in planar orientation of C_8 HET ($T = 75^\circ\text{C}$) at $t = 18$ h 30 min and (b) in homeotropic orientation of C_8 HET ($T = 75^\circ\text{C}$) at $t = 40$ h.

optical method [1], but for another dye (a yellow one), the 4-phenylazophenol, are brought together in table 3. Their comparison with the present results leads to the following remarks:

- (i) The diffusion anisotropy ratio r is always superior to 1, whatever the dyes or the mesophases considered. This value is in good agreement with previous results which have allowed to determine the structure of studied columnar discotic liquid

Table 2. Measurements of red dye diffusion coefficients D_{\perp} and D_{\parallel} for the D_h (C_8 HET) and D_0 (C_{11} HAT) phases by the 'mirage effect' method.

Sample	$T/^{\circ}\text{C}$	$D_{\perp}/\text{m}^2\text{s}^{-1}$	$D_{\parallel}/\text{m}^2\text{s}^{-1}$	D_{\parallel}/D_{\perp}
C_8 HET	75	1.24×10^{-9}	1.61×10^{-9}	1.3
C_{11} HAT	90	4.61×10^{-9}	10.96×10^{-9}	2.4

Table 3. Measurements of yellow dye diffusion coefficients D_{\perp} and D_{\parallel} for the D_h (C_8 HET) and D_2 (C_{11} HAT) phases by optical method, presented in [1].

Sample	$T/^{\circ}\text{C}$	$D_{\perp}/\text{m}^2\text{s}^{-1}$	$D_{\parallel}/\text{m}^2\text{s}^{-1}$	D_{\parallel}/D_{\perp}
C_8 HET	75	1.75×10^{-9}	1.93×10^{-9}	1.1
C_{11} HAT	115	9.96×10^{-9}	21.90×10^{-9}	2.2

crystals, liquid-like order along the column direction and solid-like order perpendicularly to it.

- (ii) The diffusion anisotropy ratio is larger for the C_{11} HAT ($r = 2.4$) than the C_8 HET one ($r = 1.3$). This is probably due to the difference in the length and type of the aliphatic chains bound to the triphenylene discs ($-\text{OCO}-C_{11}H_{23}$ and $-\text{O}-C_8H_{17}$). In fact, the inter-columnar distances for the two mesophases, increase from 2.22 nm for the C_8 HET to 2.66 nm for the C_{11} HAT. More, unlike ethers, the ester chains of the C_{11} HAT are not in the plane of the disc, the oxygen atoms of carboxylic group lying on both sides of the disc plane.
- (iii) The diffusion coefficient values for the red dye are inferior to those obtained for the yellow one. Their ratio varies approximately in the same proportions. For the C_8 HET, for instance, at the same temperature, we obtain

$$\frac{D_{\perp}(\text{red dye})}{D_{\perp}(\text{yellow dye})} \approx \frac{D_{\parallel}(\text{red dye})}{D_{\parallel}(\text{yellow dye})} \approx 0.75.$$

This value is nearly the same as the dye molecular diameter ratio, about 0.6. This result shows that the matter diffusion in columnar discotic mesophases decreases with the dye molecular size.

- (iv) The D_0 and the D_2 phases of C_{11} HAT have not the same diffusion coefficients although they present an hexagonal lattice. We note that these coefficients increase, for the two configurations, approximately in the same proportion:

$$\frac{D_{\perp}(\text{phase } D_2)}{D_{\perp}(\text{phase } D_0)} \approx \frac{D_{\parallel}(\text{phase } D_2)}{D_{\parallel}(\text{phase } D_0)} \approx 2.$$

This effect can be explained by the increasing of the temperature (90°C in the D_0 phase and 115°C

in the D_2 one), and by the stacking order of discs in columns. In fact, the molecules of the D_2 phase are not regularly spaced in each columns whereas the strong correlation length of molecules (a few tenths molecules) in adjacent columns gives an ordered D_0 phase [14, 15].

5. Conclusion

We have shown that the photothermal deflection technique ('mirage effect') is sensitive to the concentration variation of the dye diffusion in hexagonal columnar discotic phases for the two orientations of molecular columns. The anisotropic diffusion behaviour of matter can be measured for these kinds of samples.

In particular, this method allows us to determine the effects of the dye molecule size, of the length and shape of chains bound to the triphenylene discs, and of the stacking order or disorder of discs in columns. We can conclude that the photothermal deflection technique can be useful to characterize the matter diffusion in columnar discotic mesogens.

References

- [1] DAOUD, M., GHARBA, M., and GHARBI, A., 1994, *J. Phys. II France*, **4**, 989.
- [2] DAOUD, M., GHARBA, M., GHARBI, A., and DESTRADE, C., (submitted to *Surf. Sci. Lett.*).
- [3] BOCCARA, A. C., FOURNIER, D., and BADOZ, J., 1980, *Appl. Phys. Lett.*, **36**, 130.
- [4] BOCCARA, A. C., FOURNIER, D., JACKSON, W., and AMER, N. M., 1980, *Opt. Lett.*, **5**, 377.
- [5] SALAZAR, A., SANCHEZ-LAVEGA, A., and FERNANDEZ, J., 1991, *J. appl. Phys.*, **69**, 1223.
- [6] LEPOUTRE, F., BOUCHOULE, S., BACKSTRÖM, G., and BALAGEAS, D., 1992, in *Photoacoustic and Photothermal Phenomena III*, Vol. 69 Springer-Verlag Series in Optical Sciences, edited by D. Bicanic (Springer-Verlag, Berlin), p. 664.
- [7] HADJ-SAHARAOU, A., LOUIS, G., MANGEOT, B., PERETTI, P., and BILLARD, J., 1991, *Phys. Rev. A*, **44**, 5080.
- [8] GHARBA, M., HADJ-SAHARAOU, A., LOUIS, G., GHARBI, A., and PERETTI, P., 1990, in *Photoacoustic and Photothermal Phenomena II*, Vol. 62 Springer-Verlag Series in Optical Sciences, edited by J. C. Murphy, J. W., Maclachlan Spicer, L. C. Aomodt and B. S. H. Royce (Springer-Verlag, Berlin), p. 306.
- [9] CARSLAW, H. S., and JAEGER, J. C., 1959, *Conduction of Heat in Solids* (Oxford University Press, Oxford).
- [10] VAEZ IRAVANI, M., and NIKOONAHAD, M., 1987, *J. appl. Phys.*, **62**, 4065.
- [11] QUÉLIN, X., PERRIN, B., LOUIS, G., and PERETTI, P., 1993, *Phys. Rev. B*, **48**, 3677.
- [12] ROSENCWAIG, A., and GERSHO, A., 1976, *J. appl. Phys.*, **47**, 64.
- [13] DESTRADE, C., TINH, N. H., GASPAROUX, H., MALTHETE, J., and LEVELUT, A. M., 1981, *Molec. Cryst. liq. Cryst.*, **71**, 111.
- [14] LEVELUT, A. M., 1983, *J. chem. Phys.*, **80**, 149.
- [15] FONTES, E., HEINEY, P. A., and DE JEU, W. H., 1988, *Phys. Rev. Lett.*, **61**, 1202.